Chemical Science

ROYAL SOCIETY OF CHEMISTRY

EDGE ARTICLE

View Article Online
View Journal | View Issue



Cite this: *Chem. Sci.*, 2024, **15**, 18196

All publication charges for this article have been paid for by the Royal Society of Chemistry

# Encapsulated TADF macrocycles for high-efficiency solution-processed and flexible organic light-emitting diodes†

Xinxin Ban, *[ab] Qingpeng Cao,[a] Wenhao Zhang,[a] Wenzhong Bian,[a] Caixia Yang,[a] Jiayi Wang,[a] Youqiang Qian,[a] Hui Xu,[a] Chuanzhou Tao *[a] and Wei Jiang *[b]

Received 6th July 2024
Accepted 5th September 2024

DOI: 10.1039/d4sc04487h

rsc.li/chemical-science

Macrocyclic thermally activated delayed fluorescence (TADF) emitters have been demonstrated to realize high efficiency OLEDs, but the design concept was still confined to rigid π-conjugated structures. In this work, two macrocyclic TADF emitters, Cy-BNFu and CyEn-BNFu, with a flexible alkyl chain as a linker and bulky aromatic hydrocarbon wrapping units were designed and synthesized. The detailed photophysical analysis demonstrates that the flexible linker significantly enhances the solution-processibility and flexibility of the parent TADF core without sacrificing the radiative transition and high PLQY. Moreover, benefiting from sufficient encapsulation of both horizontal and vertical space, the macrocyclic CyEn-BNFu further isolated the TADF core and inhibited the aggregation caused quenching, which benefits the utilization of triplet excitons. As a result, the non-doped solution-processed OLEDs based on CyEn-BNFu exhibit high maximum external quantum efficiencies (EQE) up to 32.3%, which were 3 times higher than those of the devices based on the parent molecule. In particular, these macrocyclic TADF emitters ensure the fabrication of flexible OLEDs with higher brightness, color purity and bending resistance. This work opens a way to construct macrocyclic TADF emitters with a flexible alkyl chain linker and highlights the benefits of such encapsulated macrocycles for optimizing the performance of flexible solution-processed devices.



## 1 Introduction

Luminescent macrocyclic molecules with a variety of artificial structures have been widely applied in chemical sensors, supramolecular assembly, host–guest chemistry, bioimaging and electroluminescence fields.[1–8] Among the reported series of macrocyclic organic fluorophores, macrocyclic thermally activated delayed fluorescence (TADF) emitters have attracted considerable attention in recent years due to their tunable photophysical properties, high quantum yields, and 100% exciton utilization, and have the potential to significantly improve the device efficiency of organic light emitting diodes (OLEDs).[9–11] Compared to the traditional linear TADF design structure with a large dihedral angle linked electron donor and acceptor,[12–16] macrocyclization has been clearly demonstrated to be an effective strategy to suppress the non-irradiative pathways and simultaneously enhance the triplet up-conversion of reverse intersystem crossing (RISC).[17] Takeda *et al.* reported the π-conjugated macrocyclic TADF emitter and compared the device performance with its linear analog and the higher external quantum efficiency (EQE) of the device was attributed to the reduction in the non-radiative transition due to the rigid structure of the macrocyclic TADF emitter.[18] Su *et al.* also developed a series of macrocyclic TADF emitters and demonstrated that except for the rigid cyclic structure, the ideal structure, reasonable building block and horizontal dipole orientation will further distinguish the performance of the macrocyclic material.[19] However, due to the limited report of TADF macrocycles, the molecular design law and specific properties are still unclear. Thus, it is scientifically significant to extend the construction strategy and enrich the multifunction property of macrocyclic TADF materials.

Usually, most fluorescent materials suffer from two quenching effects.[10–22] One is a non-radiative transition induced by the vibration of the molecular skeleton.[23–28] The other one is aggregation-causing quenching (ACQ) induced by intramolecular interaction in the accumulated state.[29–32] To suppress molecular vibration, the π-conjugated macrocycles are preferred to be introduced to the TADF emitter, and the positive results were achieved by the previous research.[33–35] However, such rigid planar macrocycles easily undergo serious concentration quenching due to the strong π–π stacking.[36,37] Such

[a]*School of Environmental and Chemical Engineering, Jiangsu Key Laboratory of Function Control Technology for Advanced Materials, Jiangsu Ocean University, Lianyungang, Jiangsu, China. E-mail: banxx@jou.edu.cn; taocz@jou.edu.cn*

[b]*School of Chemistry and Chemical Engineering, Southeast University, Nanjing, Jiangsu, China. E-mail: jiangw@seu.edu.cn*

† Electronic supplementary information (ESI) available. See DOI: https://doi.org/10.1039/d4sc04487h

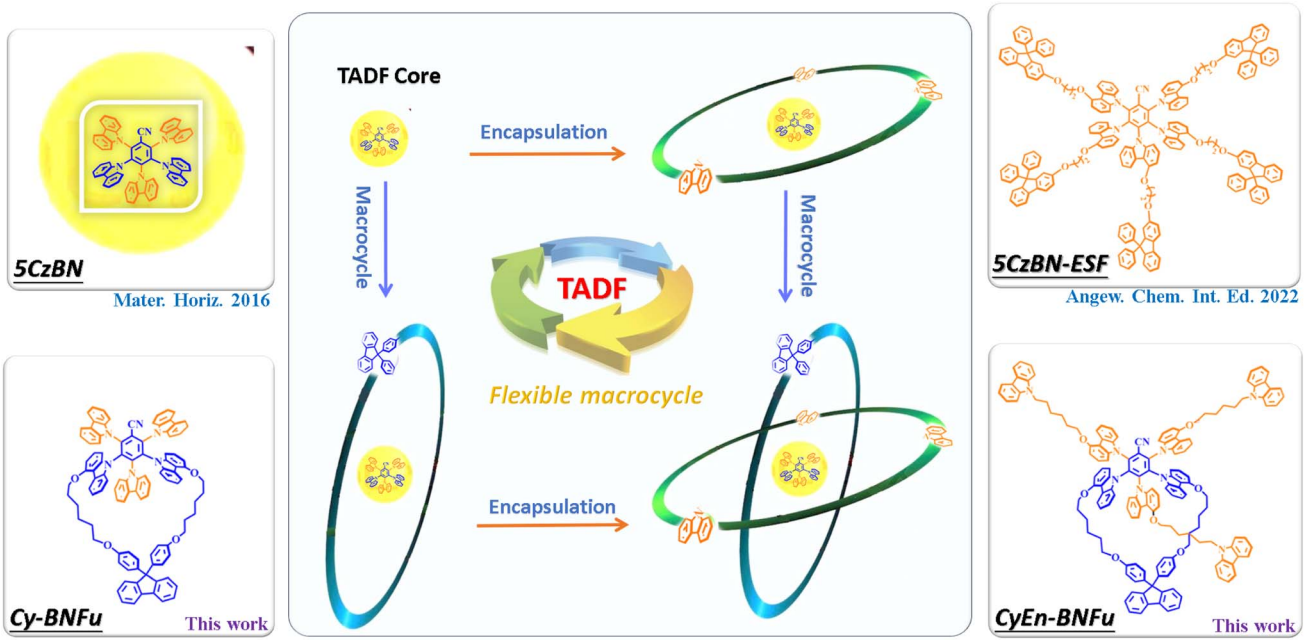


Scheme 1 Molecular structure and design strategy of flexible macrocyclic TADF materials. The horizontal cycle represents the peripheral encapsulation of carbazoles, while the vertical cycle represents the flexible alkyl chain linked fluorene.

a trade-off restricts the application range of rigid macrocyclic TADF emitters, especially in non-doped devices. That's why most of the reported macrocyclic TADF emitters needed doping into a suitable host to achieve high EQE. Meanwhile, organic semiconductors are developing in the direction of flexibility, low cost, and easy processability.[38–40] However, the relatively rigid macrocycles often restrict the movement and deformation of molecular motifs, which were not beneficial for offsetting external stress. Such rigid structures are inevitably restricted to low molecular flexibility and solubility and simultaneously limit their practical applications in solution-processed flexible OLEDs.[41] Therefore, developing an applicable strategy to construct flexible macrocyclic TADF materials with enhanced exciton utilization as well as high flexibility and solubility is highly desirable and remains a great challenge.

In this work, we demonstrate a concise and effective method to achieve a macrocyclic TADF emitter for host-free OLEDs, which minimizes the intermolecular interaction induced quenching and boosts the triplet exciton utilization while retaining the advantage of flexibility. The key feature of such a macrocycle is the incorporation of both vertical and horizontal encapsulation architecture into the TADF, which enables not only a decrease in nonradiative transition but also a substantial increase in device efficiency. By using CyEn-BNFu as the emissive layer, an ultrahigh EQE of 32.3% was achieved for host-free OLEDs, which is among the highest efficiencies for solution-processed devices. Moreover, the macrocycle with a flexible linker strategy is qualified for flexible OLEDs and ensures that the device has a high resistance to flexural strain under repeated bending. These features show that the flexible encapsulated TADF macrocycle offers a great advantage for solution-processed and host-free flexible technologies, which will enhance the performance of flexible displays and lighting in the future.

## 2. Results and discussion

Molecular encapsulation has been widely used to minimize aggregation-caused quenching by spatially isolating individual chromophores. In the past, most encapsulated materials have been prepared *via* conjugated or non-conjugated bulky side groups, which can significantly suppress intermolecular interactions. However, this approach mostly expands out through the molecular plane, which will not sufficiently limit electronic communication through the vertical direction of molecules.

If both horizontal and vertical directions are protected by bulky units, that will be helpful to the electroluminescence. We choose classical 5CzBN as the emissive TADF core to investigate the encapsulation strategies (Scheme 1). Cy-BNFu was designed with a vertical flexible macrocycle to encapsulate the TADF core, while CyEn-BNFu introduced three other branches in its horizontal direction. The molecular structure was optimized by density functional theory (DFT) at the B3LYP theory level with the 6-31G(d) basis set. As shown in Fig. 1, the alkyl carbazoles look like propellers distributed around the periphery of the TADF core, which can effectively wrap the plane direction. In addition, the diphenyl fluorene linked by the alkyl chain forms a vertical wrapping circle perpendicular to the molecular plane. Such a flexible macrocycle not only endows the TADF core with three-dimensional encapsulation, but also partly restricts the rotation of the carbazole unit, which will be helpful to the radiative transition of excited excitons. The oscillator strength value of CyEn-BNFu was higher than that of Cy-BNFu after introducing a bulky fluorene macrocycle. Similar to the

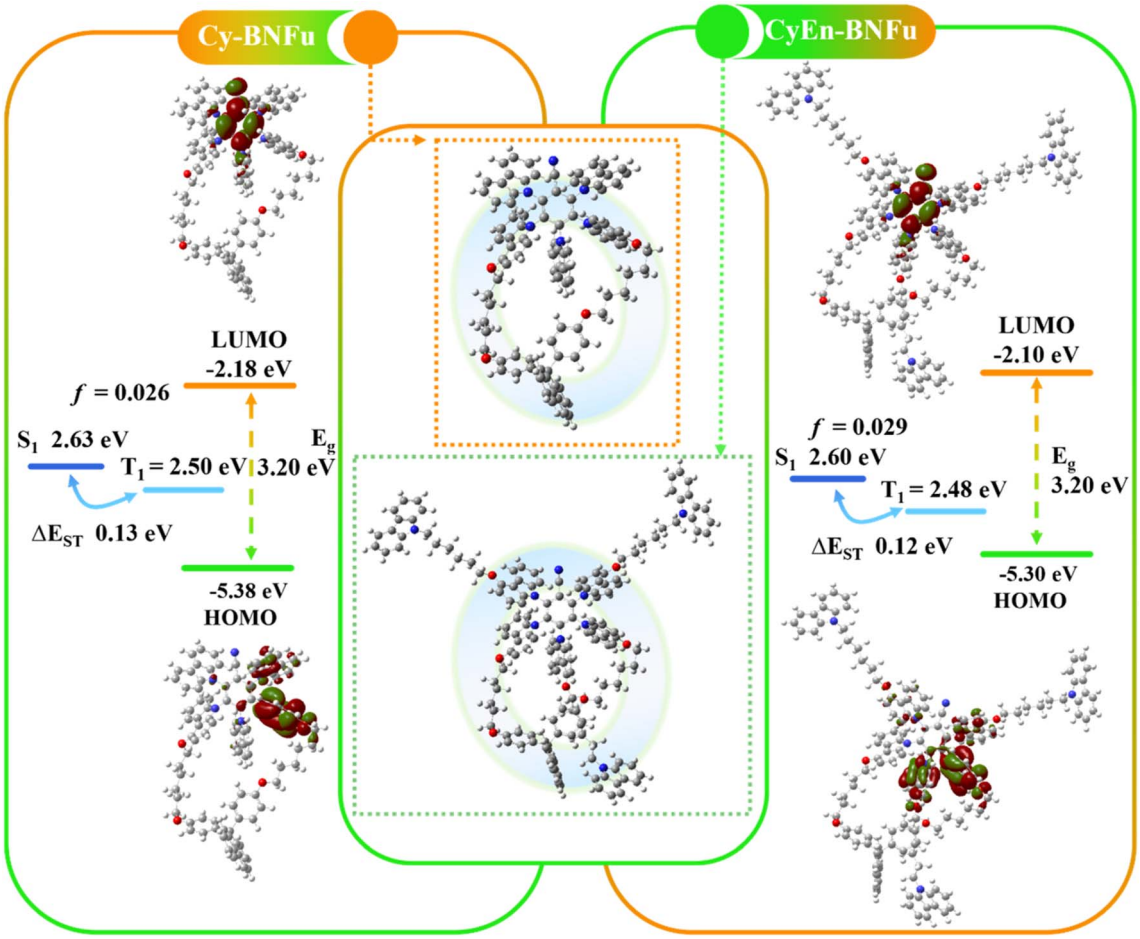


Fig. 1 Optimized geometries and electron cloud distribution maps of Cy-BNFu and CyEn-BNFu.

emissive core, the lowest unoccupied molecular orbitals (LUMOs) were concentrated on the benzyl cyanide unit owing to its strong electron-withdrawing properties, while the highest occupied molecular orbitals (HOMOs) were mainly distributed on the carbazole units of the emissive core. The calculated HOMO and LUMO energy levels are −5.38/−2.18 eV and −5.30/−2.10 eV for Cy-BNFu and CyEn-BNFu, respectively. The obviously separated frontier orbital illustrates a small charge exchange integral, which will result in a small singlet and triplet splitting ($\Delta E_{ST}$). By calculating with time-dependent DFT (TD-DFT), the singlet ($S_1$) and triplet ($T_1$) state energies were found to be 2.63/2.50 eV and 2.60/2.48 eV, respectively. The $\Delta E_{ST}$ of Cy-BNFu and CyEn-BNFu was calculated to be 0.13 eV and 0.12 eV, respectively. Such a small $\Delta E_{ST}$ will promote the efficient triplet up-conversion process and subsequently efficient TADF emission. Obviously, no electronic signature was distributed to the peripheral carbazole or fluorene units due to the insulated alkyl chain. The introduction of bulky functional dendritic units at the periphery of the emissive core can suppress the intermolecular interaction without disturbing the electronic properties of the emissive core, which means the peripheral carbazole and fluorene was only used as wrapping units and will not extend π-conjugation. Indeed, the following photoluminescence spectra demonstrate that the commercially available carbazole and fluorene constructed macrocyclic TADF emitters can enhance the PLQY and suppress the bathochromic shift of spectra in the solid film. The non-conjugated linking keeps the TADF properties unchanged and ensures that the emitter is more effective for solution processibility, which indicates the macrocycle encapsulation will significantly influence the electroluminescence properties of the material.

Fig. 2a and b present the UV-vis absorption and photoluminescence spectra of Cy-BNFu and CyEn-BNFu diluted in toluene. Both of the two compounds exhibit similar absorption including intense peaks at 320 and 340 nm, which are attributed to the π–π* and n–π* transitions of conjugated benzene and carbazole units. The broad absorption band around 400 nm was assigned to the charge transfer transition from the carbazole to the benzonitrile fragment. The optical band gaps ($E_g$) of Cy-BNFu and CyEn-BNFu were calculated to be 2.77 and 2.75 eV from the onset absorption. The absorption of CyEn-BNFu is sharper and more well-resolved compared to Cy-BNFu, indicating lower conformational disorder in the ground state due to the better wrapping properties of such macrocycle encapsulation. The PL spectra in toluene of the two macrocycles peaked around 470 nm with intense green emission, which means

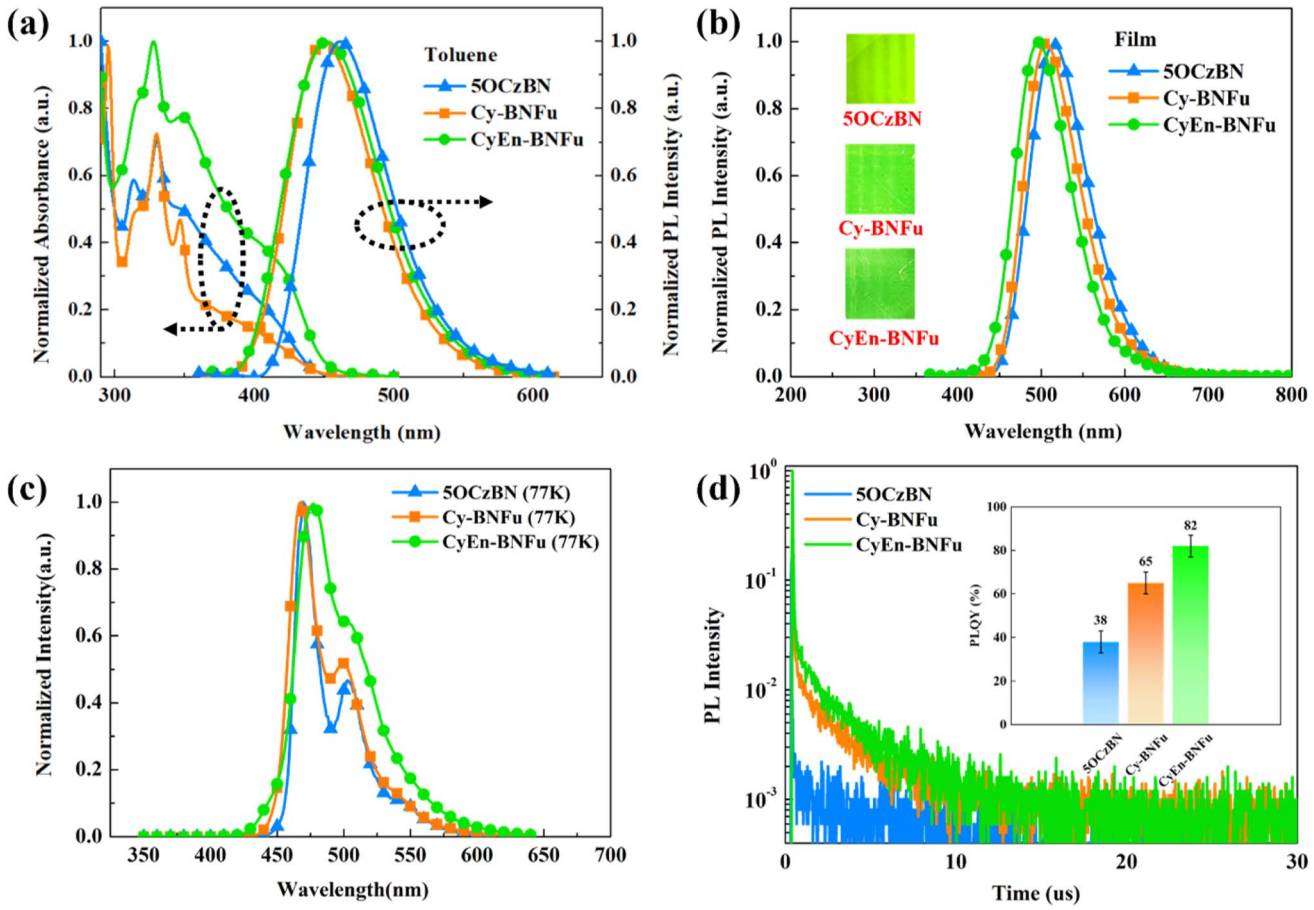


Fig. 2 (a) UV-vis absorption and PL emission of 5OCzBN, Cy-BNFu and CyEn-BNFu in toluene ($10^{-4}$ M) at room temperature. (b) PL emission of 5OCzBN, Cy-BNFu and CyEn-BNFu in toluene states. (c) Phosphorescence spectra at 77 K of 5OCzBN, Cy-BNFu and CyEn-BNFu in toluene ($10^{-4}$ M). (d) Transient PL spectra of 5CzBN, Cy-BNFu and CyEn-BNFu in the pure films (the inset shows the PLQY of 5OCzBN, Cy-BNFu and CyEn-BNFu in pure films).

a similar 0–1 transition in diluted solution with isolated molecules. However, the solid film state exhibits distinct PL spectra of different wrapping strategies. The TADF core 5OCzBN without any encapsulation shows a broad and red-shifted PL spectrum with the formation of lower energy species at the emission tail due to the significant molecular accumulation. After introducing vertical macrocyclic encapsulation, the PL spectrum of Cy-BNFu gradually blue shifted to 505 nm, indicating some remnant intermolecular interaction. Further equipping with horizontal wrapping, CyEn-BNFu exhibits an emission at 495 nm with a decreased peak width at half height. Moreover, the PLQYs of the Cy-BNFu and CyEn-BNFu were characterized to be 65% and 82%, respectively. Even with the same fraction of TADF units, the PLQY of 5OCzBN was only 38%. These observations fully demonstrate that the macrocyclic encapsulation can effectively suppress intermolecular interactions and thus enhance the photoluminescence properties. The singlet ($S_1$) and triplet ($T_1$) energy levels of Cy-BNFu and CyEn-BNFu were determined by the fluorescence at 300 K and phosphorescence spectra at 77 K, respectively. As shown in Table 1 and Fig. 2c, their $S_1$ energy levels are 2.95 and 2.94 eV, while the $T_1$ energy levels are 2.78 and 2.80 eV, which result in small $\Delta E_{ST}$ of 0.17 and 0.14 eV for Cy-BNFu and CyEn-BNFu, respectively. The HOMO energy levels of Cy-BNFu and CyEn-BNFu were estimated to be −5.72 and −5.70 eV by cyclic voltammetry (CV) experiments (Fig. S2, ESI†), while the LUMO energy level was −2.95 eV for both Cy-BNFu and CyEn-BNFu deduced from the HOMO and $E_g$. The comparable HOMO and LUMO energy levels of the two macrocycles are consistent with the conclusions of the aforementioned theoretical computation.

The transient PL spectra of Cy-BNFu and CyEn-BNFu are recorded to evaluate the excited photophysical properties. As shown in Fig. 2d, the distinct prompt fluorescence ($\tau_p$) with nanosecond-order and delayed fluorescence emission ($\tau_d$) with microsecond-order demonstrate the TADF properties of the two macrocycles. The $\tau_p$ values of Cy-BNFu and CyEn-BNFu are 33 ns and 35 ns, while their delayed fluorescence emission $\tau_d$ are 1.59 μs and 2.68 μs, respectively. To quantificationally compare the difference of molecular exciton kinetics, photophysical parameters were precisely calculated (Table S1†). The calculated rate constants of the RISC process ($k_{RISC}$) are remarkably increased from $2.77 \times 10^6$ $s^{-1}$ for Cy-BNFu to $2.92 \times 10^6$ $s^{-1}$ for CyEn-BNFu, which means vertical encapsulation giving rise to increased delayed fluorescence. Moreover, the nonradiative

Table 1 Physical and electrochemical properties of Cy-BNFu and CyEn-BNFu

| Sample | $T_d/T_g$ (°C) | UV[a] (nm) | PL (nm) | $E_g$ (eV) | $S_1/T_1$ (eV) | $\Delta E_{ST}$ (eV) | HOMO (eV) | LUMO (eV) |
|---|---|---|---|---|---|---|---|---|
| Cy-BNFu | 428/215 | 329, 292 | 472[a] | 2.77[c] | 2.95/2.78[e] | 0.17[e] | −5.72[f] | −2.95[g] |
| | | | 505[b] | 3.20[d] | 2.63/2.50[d] | 0.13[d] | −5.38[d] | −2.18[d] |
| CyEn-BNFu | 411/143 | 330, 295 | 475[a] | 2.75[c] | 2.94/2.80[e] | 0.14[e] | −5.70[f] | −2.95[g] |
| | | | 495[b] | 3.20[d] | 2.60/2.48[d] | 0.12[d] | −5.30[d] | −2.10[d] |

[a] Measured in toluene solution at room temperature. [b] Measured in thin film at room temperature. [c] Optical energy gap values estimated from the UV absorption edge. [d] Gaussian simulation. [e] Estimated in toluene at 77 K. [f] Determined by cyclic voltammetry in $CH_2Cl_2$. [g] Deduced from the HOMO and $E_g$.

decay rates of CyEn-BNFu triplet excitons $k_{nr}^T$ were decreased to 0.74 $\times 10^5$ $s^{-1}$ compared to 2.54 $\times 10^5$ $s^{-1}$ for Cy-BNFu. Meanwhile, thanks to the enhanced vibronic coupling, the higher $k_{RISC}$ and low $k_{nr}^T$ of CyEn-BNFu demonstrate the enhanced up-conversion process of triplet excitons ($T_1 \rightarrow S_1$) and suppressed triplet exciton concentration quenching of the encapsulated macrocycle. As a result, the flexible cycle constructed by alkyl chain wrapping can isolate the aggregation-induced electronic quenching and enhance the effective triplet exciton utilization of CyEn-BNFu, which would be beneficial to its electroluminescence.

The solubility, thermal stability and film forming ability are extremely important in solution-processed OLED devices. As shown in Fig. 3a, the macrocycle can easily dissolve in most common solvents such as ethyl acetate, dichloroethane, chlorobenzene, tetrahydrofuran and dimethylformamide. In

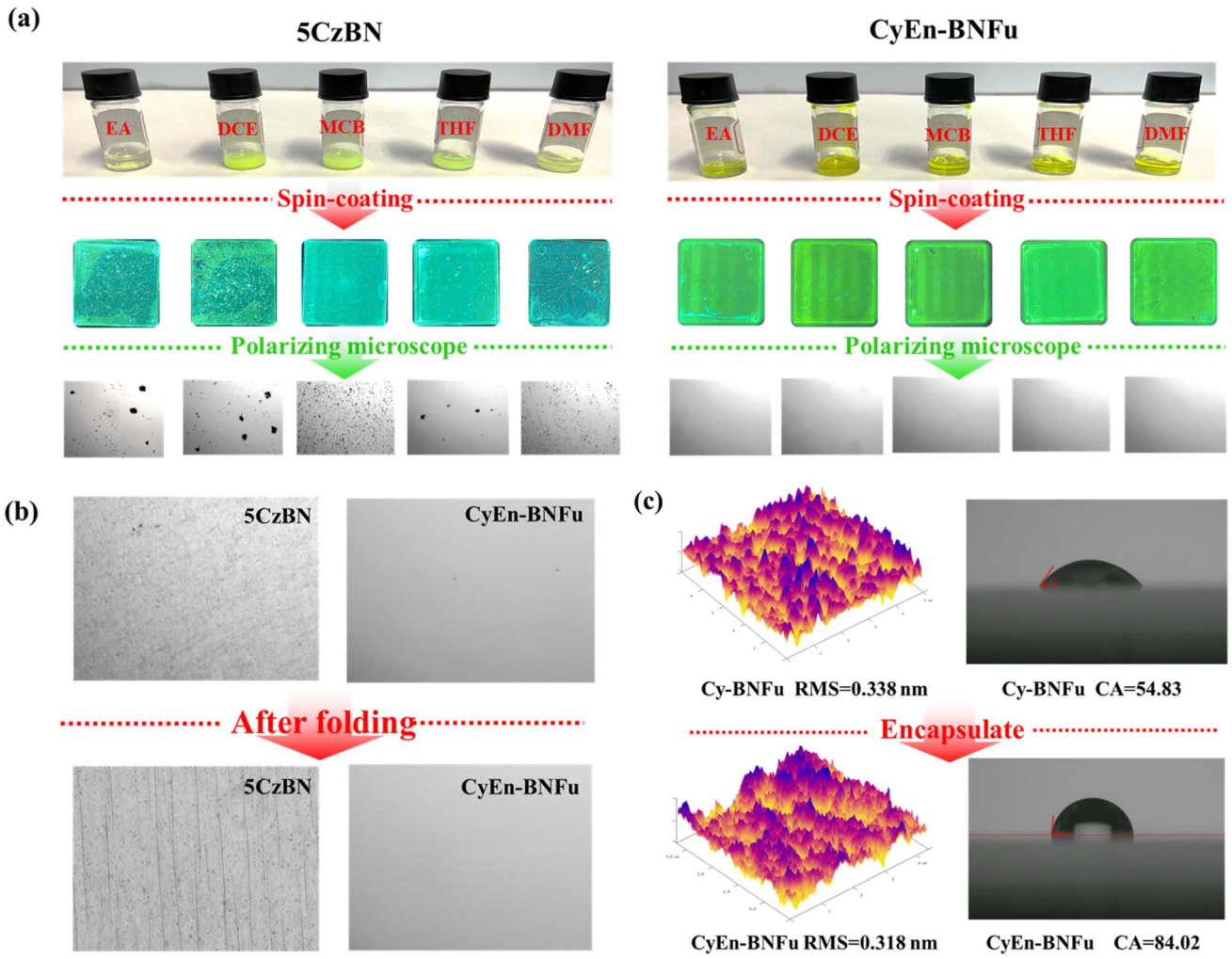


Fig. 3 (a) Images of dissolution of 5CzBN and CyEn-BNFu in different solvents (EA = ethyl acetate, DCE = dichloroethane, MCB = monochlorobenzene, THF = tetrahydrofuran, DMF = *N*,*N*-dimethylformamide); spin-coating pictures and corresponding polarized light microscope images. (b) Polarized light microscopy images of 5CzBN and CyEn-BNFu before and after bending. (c) Atomic force microscope (AFM) images and contact angles of Cy-BNFu and CyEn-BNFu.

contrast, the rigid parent TADF core 5CzBN is difficult to dissolve in these solvents even with heating or ultrasound. The poor solubility of 5CzBN significantly influences the film forming properties. As shown under the microscope, the spin-coated 5CzBN film on ITO glass exhibits many large particles and cracks, while the encapsulated macrocycle shows a uniform and flat film. To demonstrate the good film morphology, atomic force microscopy (AFM) was performed (Fig. 3c). It is found that both Cy-BNFu and CyEn-BNFu achieve small root-mean-square (RMS) roughness of 0.338 and 0.318 nm without any particle aggregation or cracks.

The bending resistance is also an important factor for solution-processible materials used for flexible OLEDs. Both the macrocycle and its parent emission core are spin-coated on a PET substrate. As shown in Fig. 3b, after bending 100 times, 5CzBN underwent severe film cracking and wrinkling phenomena, while CyEn-BNFu still maintains its original flatness and uniformity, which indicates the encapsulation with flexible alkyls also enhanced the durability of the flexible emission film. The contact angles for the two macrocycles are also investigated and the encapsulated CyEn-BNFu exhibits more hydrophobicity with contact angles of 84.02° after introducing the alkyl chain, which means the flexible alkyl chain around the TADF core will also help to prevent water intrusion. Thermogravimetric analysis (TGA) and differential scanning calorimetry (DSC) measurements were then carried out. As shown in Fig. S1,† Cy-BNFu and CyEn-BNFu show high decomposition temperatures ($T_d$, defined as 5% weight loss in TGA measurement) of 428 °C and 411 °C, respectively, guaranteeing their stable processing during thermal annealing. Meanwhile, from DSC measurements in the range from 30 °C to 300 °C, both Cy-BNFu and CyEn-BNFu exhibit very high glass transition temperatures ($T_g$) of 143 °C to 215 °C, respectively. All these above results verify that flexible macrocyclic TADF is promising for developing high-performance solution-processed OLEDs.

To evaluate Cy-BNFu and CyEn-BNFu emitters for host-free OLEDs, electroluminescent (EL) devices with the architecture of ITO/PEDOT:PSS (40 nm)/emitters (40 nm)/TPBi/(40 nm)/$Cs_2CO_3$ (1 nm)/Al (100 nm) were fabricated (Fig. 4a). The typical PEDOT:PSS and TPBi serve as the hole injection layer and the electron-transporting layer, respectively. In accordance with PL spectra, the EL peaks of Cy-BNFu and CyEn-BNFu are 523 and 515 nm; the blue-shifted and narrow FWHM can be assigned to the increased encapsulation degree, which is consistent with the PL spectra (Table S2†). Without encapsulation, the TADF core exhibits a severe redshifted and widened spectrum due to the accumulated excitons and severe quenching effect by the intermolecular interaction. The current density–voltage–luminance (*J–V–L*) characteristics, EQE *versus* current density curves, and EL spectra for devices are depicted in Fig. 4c and d, and the EL data are summarized in Table 2. The CyEn-BNFu-based device gave a lower turn-on voltage of 3.6 V than that of Cy-BNFu, which could be partly ascribed to the shallow HOMO of CyEn-BNFu. The parent TADF core exhibits unsatisfactory device efficiency with a maximum EQE of only 9.4% due to severe intermolecular interaction induced concentration quenching. After cyclic wrapping from the vertical direction, the Cy-BNFu-based device displays clearly improved EL performances with the maximum $EQE_{max}$, current efficiency ($CE_{max}$) and power efficiency ($PE_{max}$) of 12.4%, 37.1 cd $A^{-1}$ and 16.6 lm $W^{-1}$, respectively. The far higher maximum EQE than that of naked materials clearly presents a proof-of-concept of the encapsulated macrocyclic TADF emitter for high OLEDs. Importantly, the CyEn-BNFu-based device displayed high $EQE_{max}$, $CE_{max}$ and $PE_{max}$ of 32.3%, 95.8 cd $A^{-1}$ and 66.9 lm $W^{-1}$, respectively. Given the comparable emissive structures and device architectures, the gradually enhanced device efficiency of the vertical macrocycle and encapsulated macrocycle can be attributed to the suppression of the intermolecular interaction induced exciton quenching of the host-free emission layer. Moreover, the higher efficiency of CyEn-BNFu than Cy-BNFu also indicates that only single directional wrapping cannot completely isolate the electronic interaction between adjacent emissive cores. These results demonstrate the macrocycle encapsulation by the flexible alkyl chain could serve as a promising strategy to develop highly efficient TADF emitters.

To further investigate the effect of macrocycle encapsulation for the host-free devices, the emitting layer (EML) is composed of the TADF molecule dispersed into CBP (4,4′-bis(*N*-carbazolyl)-1,1′-biphenyl) at different doping concentrations of 20, 30 and 40 wt%. Since Cy-BNFu was not fully encapsulated, the EL spectra gradually red shifted with the increasing doping concentration. Moreover, the peak EQE is monotonically increased from 10.5% to 11.4% to 25.3% for the doping concentrations of 20, 30 and 40 wt%, respectively (Fig. 4e and f). The improved device efficiency indicates exciton quenching still exists in the macrocyclic Cy-BNFu, which needs a host material to further isolate the emissive core and suppress the non-radiative transition. In contrast, the device performance of CyEn-BNFu gradually decreased with the introduction of CBP as a host. The non-doped CyEn-BNFu achieved the highest efficiency which means the macrocycle encapsulation has already achieved a suitable stereo-structure, and the additional host will further increase the distance to the luminescent core, which may not be helpful for carrier balance and exciton utilization. This trend is in agreement with most of the reports that each TADF emitter has its appropriate doping concentration to achieve the best device performance. As for the encapsulation strategy, the degree of encapsulation will also affect the efficiency of TADF emitters. These results clearly demonstrate that a flexible encapsulated macrocycle ensures that CyEn-BNFu will produce a significant improvement in overall performances for host-free solution-processed OLEDs. This strategy will further expand the design concept of the TADF material and increase the macrocyclic material system.

Flexible OLEDs are attracting tremendous attention due to their promise as a key element in bendable display and curved lighting applications (Fig. 5). In view of the high efficiency for host-free devices based on CyEn-BNFu, this flexible macrocycle was also used to fabricate flexible OELDs based on a PET substrate. The flexible device achieves a maximum EQE of 13.6% and CE of 43.6 cd $A^{-1}$, which is a record performance for host-free flexible OLEDs (Fig. 5b and Table S3†). However, the

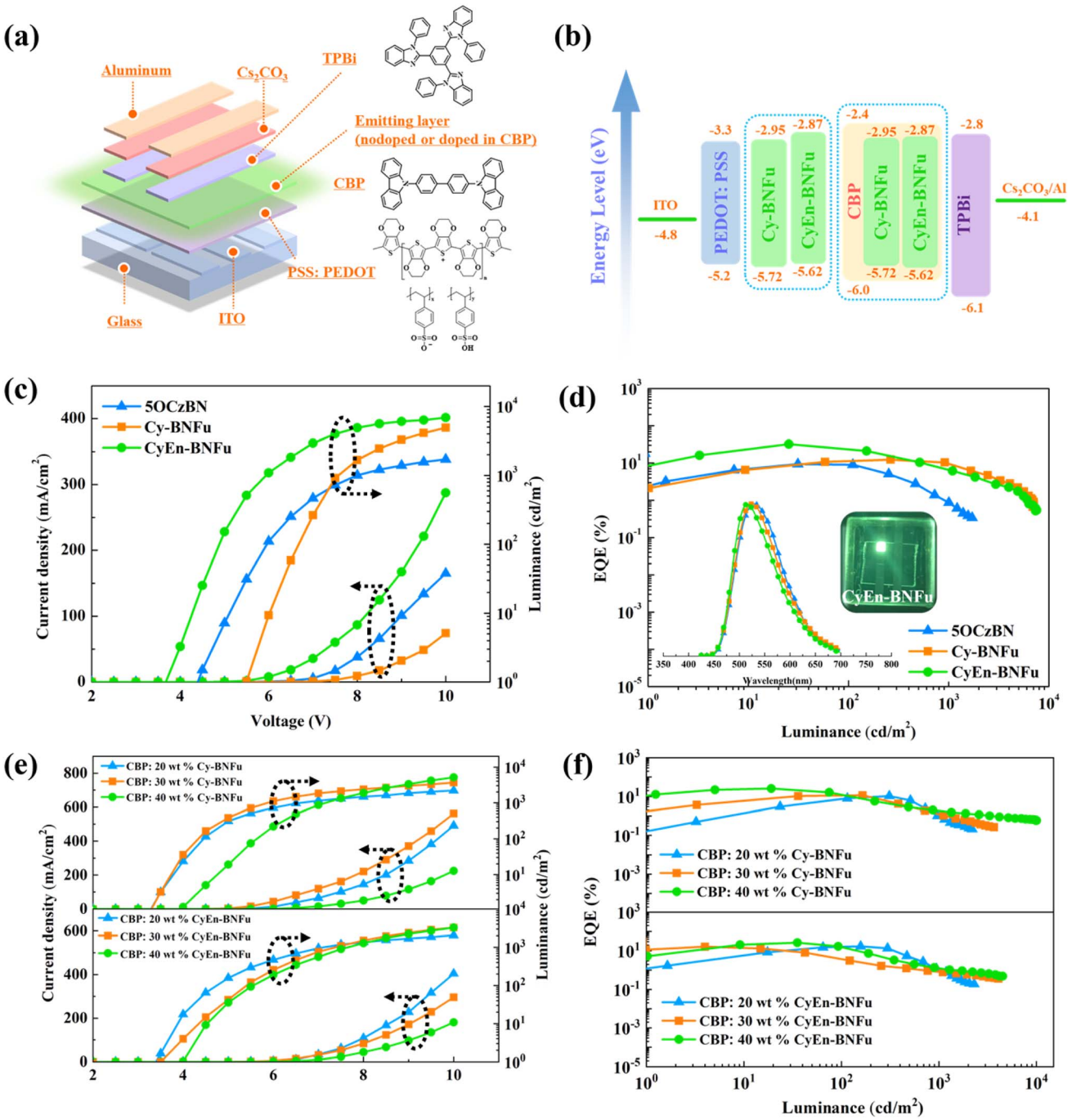


Fig. 4 (a) Layered structures of the organic light-emitting diode device and corresponding structures of the used materials. (b) Solution-processed device architecture and related energy levels. (c) Curves of current density–voltage–luminance ($J$–$V$–$L$) of the non-doped and doped devices (e). (d) Curves of EQE value *versus* current luminance (inset shows the EL spectra at 1000 cd $m^{-2}$ and the photo of the device). (f) Curves of EQE value *versus* luminance of the doped device.

rigid TADF core only exhibits a low EQE of 5.2%. To evaluate the flexibility of the OLEDs, the electroluminescence of the device was tested before and after bending at a radius of curvature ($R_c$) of 2.0 mm (Fig. 5d). The brightness of 5OCzBN decreased severely with the number of bending cycles, which may be attributed to the brittle film induced cracks and wrinkles indicated by morphological testing. In contrast, the flexible macrocyclic TADF based device exhibits a consistent high luminance without obvious decrease, which demonstrates that this flexible macrocyclic material can resist such bending in OLEDs. Even upon bending the device to a sharp angle, the device still exhibits a high luminance of 3400 cd $m^{-2}$, which means the flexible OLEDs still work very well. These results verify that the flexible encapsulated macrocycle enables not only high efficiency but also good flexibility in practical applications of flexible OLEDs.

Table 2 Device performance data of TADF-OLEDs

| Emission layer | $V_{on}$[a] [V] | $CE_{max}$[b] [cd $A^{-1}$] | $PE_{max}$[c] [lm $W^{-1}$] | $EQE_{max}$[d] [%] | $L_{max}$[e] [cd $m^{-2}$] | CIE[f] [$x$, $y$] |
|---|---|---|---|---|---|---|
| 5OCzBN | 4.4 | 28.9 | 16.5 | 9.4 | 1710 | (0.34, 0.58) |
| Cy-BNFu | 5.4 | 37.1 | 16.6 | 12.4 | 7103 | (0.32, 0.57) |
| CyEn-BNFu | 3.6 | 95.8 | 66.9 | 32.3 | 7533 | (0.31, 0.57) |
| CBP:20 wt% Cy-BNFu | 3.4 | 24.1 | 15.1 | 10.5 | 3851 | (0.20, 0.41) |
| CBP:30 wt% Cy-BNFu | 3.4 | 28.0 | 20.2 | 11.4 | 5344 | (0.21, 0.46) |
| CBP:40 wt% Cy-BNFu | 4.0 | 72.3 | 45.4 | 25.3 | 10 039 | (0.28, 0.54) |
| CBP:20 wt% CyEn-BNFu | 3.5 | 41.8 | 26.3 | 17.1 | 3707 | (0.20, 0.40) |
| CBP:30 wt% CyEn-BNFu | 3.5 | 43.4 | 34.1 | 16.5 | 5958 | (0.23, 0.50) |
| CBP:40 wt% CyEn-BNFu | 4.0 | 73.9 | 46.4 | 26.4 | 7322 | (0.27, 0.54) |

[a] $V_{on}$ = turn-on voltage at 1 cd $m^{-2}$. [b] $CE_{max}$ = maximum current efficiency. [c] $PE_{max}$ = maximum power efficiency. [d] $EQE_{max}$ = maximum external quantum efficiency. [e] $L_{max}$ = maximum luminance. [f] CIE = the Commission Internationale de L'Eclairage coordinates.

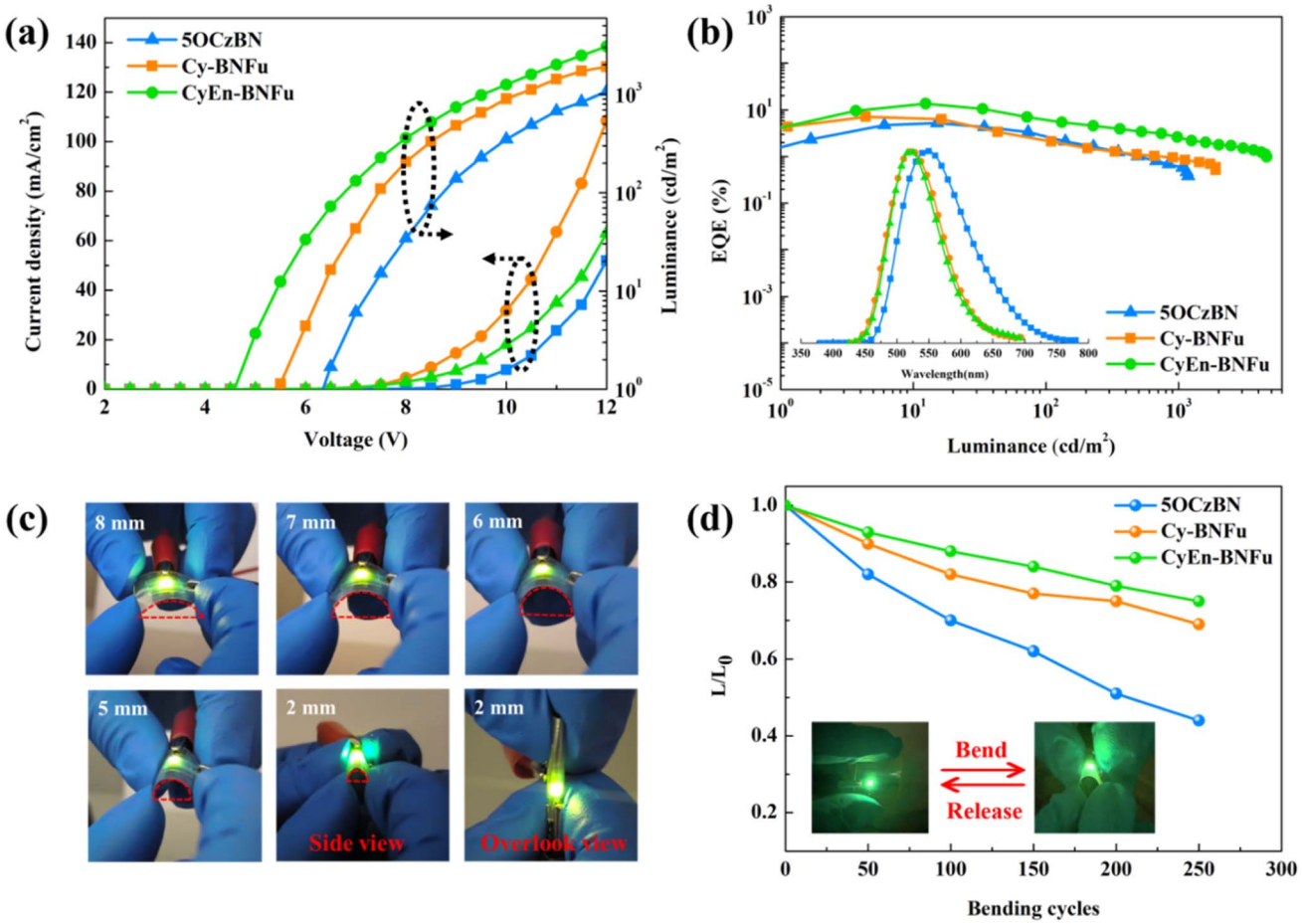


Fig. 5 (a) Current density–voltage–luminance (*J*–*V*–*L*) curves of 5OCzBN, Cy-BNFu and CyEn-BNFu OLEDs. (b) External quantum efficiency (EQE) *versus* luminance. Inset: The photo of the EL spectra. (c) Emission images of the PET-based OLED captured at high luminance (>3000 cd $m^{-2}$) under random deformation and with decreasing bending radii from 8 to 2 mm at 7 V. (d) Luminance of the flexible OLEDs as a function of the bending radius after 250 bending cycles.

## 3 Conclusion

In summary, we have developed an efficient approach to actualize the flexibility of TADF macrocycles by introducing long alkyl units in both vertical and horizontal directions, while suppressing the ACQ effect through efficient macrocycle encapsulation. The flexible macrocycle with non-conjugated linked diphenyl fluorene significantly enhances the solution-processibility without sacrificing the radiative transition and high PLQY. Furthermore, the axial propeller-like hexane carbazoles efficiently inhibit the π–π stacking of the luminant macrocycle, which leads to a more ideal encapsulation effect for

suppressing the spectral redshift and broadening. The resulting non-doped OLEDs incorporating CyEn-BNFu afforded a maximum EQE as high as 32.3%, which is among the highest efficiency of solution-processed OLEDs. Especially, this macrocyclic TADF material ensures the fabrication of flexible OLEDs with higher brightness, color purity and bending resistance. This is the first report of a flexible macrocycle encapsulated TADF emitter, and such a design strategy perfectly integrates flexibility into the macrocyclic TADF emitter for achieving both intense luminance and efficient solution-processibility, which will open a new way to construct multifunctional electroluminescent materials.

## Data availability

The data that support the findings of this study are available in the ESI† of this article.

## Author contributions

Xinxin Ban: scheme design, probe synthesis, writing – original draft. Qingpeng Cao: writing – review & editing. Wenhao Zhang: formal analysis. Wenzhong Bian: writing – review & editing. Caixia Yang: theoretical calculation. Jiayi Wang: validation, resources, writing – review & editing, supervision. Youqiang Qian: formal analysis, investigation. Hui Xu: writing – review & editing. Chuanzhou Tao: writing – review & editing. Wei Jiang: writing – review & editing, supervision.

## Conflicts of interest

The authors declare that they have no known competing financial interests or personal relationships that could have appeared to influence the work reported in this paper.

## Acknowledgements

We are grateful for the grants from the National Natural Science Foundation of China (21805106), Lianyungang Project for Transformation of Scientific and Technological Achievements (CA202103), Lianyungang 521 Funding Project (LYG06521202161), and Six Talent Peaks Project in Jiangsu Province (JNHB 114). We are also thankful for the project supported by the First-class Undergraduate Majors Construction Program of Jiangsu Province, the Postgraduate Research & Practice Innovation Program of Jiangsu Province (KYCX22_3391), and the Key Discipline Construction Program of Jiangsu Province, a Project Funded by the Priority Academic Program Development of Jiangsu Higher Education Institutions (PAPD).

## References

1 H. Y. Zhou, D. W. Zhang, M. Li and C. F. Chen, A calix[3]acridan-based host-guest cocrystal exhibiting efficient thermally activated delayed fluorescence, *Angew. Chem., Int. Ed.*, 2022, **61**(15), 202117872.

2 H. H. Cho, D. G. Congrave, A. J. Gillett, S. Montanaro, H. E. Francis, V. Riesgo-Gonzalez, J. Ye, R. Chowdury, W. Zeng, M. K. Etherington, J. Royakkers, O. Millington, A. D. Bond, F. Plasser, J. M. Frost, C. P. Grey, A. Rao, R. H. Friend, N. C. Greenham and H. Bronstein, Suppression of Dexter transfer by covalent encapsulation for efficient matrix-free narrowband deep blue hyperfluorescent OLEDs, *Nat. Mater.*, 2024, **23**, 519–526.

3 C.-M. Yu, X. Meng, X. Liu, Z.-Y. Zhang and C. Li, Switchable Supramolecular Jalousie Constructed from a Fluorenone Macrocycle, *Chem. Mater.*, 2021, **34**(1), 358–365.

4 Y. Wei, Y. Yan, X. Li, L. Xie and W. Huang, Covalent nanosynthesis of fluorene-based macrocycles and organic nanogrids, *Org. Biomol. Chem.*, 2021, **20**(1), 73–97.

5 H. Zhu, L. Chen, B. Sun, M. Wang, H. Li, J. F. Stoddart and F. Huang, Applications of macrocycle-based solid-state host–guest chemistry, *Nat. Rev. Chem*, 2023, **7**(11), 768–782.

6 B. L. Regen-Pregizer and H. Dube, Defining Unidirectional Motions and Structural Reconfiguration in a Macrocyclic Molecular Motor, *J. Am. Chem. Soc.*, 2023, **145**(24), 13081–13088.

7 B. Chen and F. Jäkle, Boron-Nitrogen Lewis Pairs in the Assembly of Supramolecular Macrocycles, Molecular Cages, Polymers, and 3D Materials, *Angew. Chem., Int. Ed.*, 2023, **63**(3), 202313379.

8 P. Zhang, Y. Zhang, L. Wang, K. Qiu, X. Tang, J. K. Gibson, X. Liu, L. Mei, S. An, Z. Huang, P. Ren, Y. Wang, Z. Chai and W. Shi, Bioinspired Macrocyclic Molecule Supported Two-Dimensional Lamellar Membrane with Robust Interlayer Structure for High-Efficiency Nanofiltration, *Adv. Sci.*, 2022, **10**(5), 2206516.

9 P. Rajamalli, F. Rizzi, W. Li, M. A. Jinks, A. K. Gupta, B. A. Laidlaw, I. D. W. Samuel, T. J. Penfold, S. M. Goldup and E. Zysman-Colman, Using the mechanical bond to tune the performance of a thermally activated delayed fluorescence emitter, *Angew. Chem., Int. Ed.*, 2021, **60**(21), 12066–12073.

10 S. Shikita, G. Watanabe, D. Kanouchi, J. Saito and T. Yasuda, Alternating Donor–Acceptor π-Conjugated Macrocycle Exhibiting Efficient Thermally Activated Delayed Fluorescence and Spontaneous Horizontal Molecular Orientation, *Adv. Photonics Res.*, 2021, **2**(7), 2100021.

11 T. Fan, Y. Zhang, L. Wang, Q. Wang, C. Yin, M. Du, X. Jia, G. Li and L. Duan, One-Shot Synthesis of B/N-Doped Calix[4]arene Exhibiting Narrowband Multiple Resonance Fluorescence, *Angew. Chem., Int. Ed.*, 2022, **61**(52), e202213585.

12 Y. Liu, J. Yang, Z. Mao, Y. Wang, J. Zhao, S.-J. Su and Z. Chi, Isomeric thermally activated delayed fluorescence emitters for highly efficient organic light-emitting diodes, *Chem. Sci.*, 2023, **14**(6), 1551–1556.

13 M. C. Tang, M. Y. Chan and V. W. Yam, Molecular Design of Luminescent Gold(III) Emitters as Thermally Evaporable and Solution-Processable Organic Light-Emitting Device (OLED) Materials, *Chem. Rev.*, 2021, **121**(13), 7249–7279.

14 N. Aizawa, Y. J. Pu, Y. Harabuchi, A. Nihonyanagi, R. Ibuka, H. Inuzuka, B. Dhara, Y. Koyama, K. I. Nakayama, S. Maeda,

F. Araoka and D. Miyajima, Delayed fluorescence from inverted singlet and triplet excited states, *Nature*, 2022, **609**(7927), 502–506.

15 X. Zhang, M. Zeng, Y. Zhang, C. Zhang, Z. Gao, F. He, X. Xue, H. Li, P. Li, G. Xie, H. Li, X. Zhang, N. Guo, H. Cheng, A. Luo, W. Zhao, Y. Zhang, Y. Tao, R. Chen and W. Huang, Multicolor hyper afterglow from isolated fluorescence chromophores, *Nat. Commun.*, 2023, **14**(1), 475.

16 T. Wang, X. Yin, X. Cao and C. Yang, A Simple Approach to Solution-Processible Small-Molecule Multi-Resonance TADF Emitters for High-Performance Narrowband OLEDs, *Angew. Chem., Int. Ed.*, 2023, **62**(24), 202301988.

17 Q. Feng, S. Zhu, B. Wang, F. Yu, H. Li, M. Yu, M. Xu and L. Xie, Thermally Activated Delayed Fluorescence Macrocycles for Organic Light-Emitting Diodes, *Adv. Funct. Mater.*, 2023, **34**(14), 2312622.

18 S. Izumi, H. F. Higginbotham, A. Nyga, P. Stachelek, N. Tohnai, P. Silva, P. Data, Y. Takeda and S. Minakata, Thermally activated delayed fluorescent donor-acceptor-donor-acceptor pi-conjugated macrocycle for organic light-emitting diodes, *J. Am. Chem. Soc.*, 2020, **142**(3), 1482–1491.

19 Y. Fu, Z. Ye, D. Liu, Y. Mu, J. Xiao, D. Hu, S. Ji, Y. Huo and S. J. Su, Macrocyclic engineering of thermally activated delayed fluorescent emitters for high-efficiency organic light-emitting diodes, *Adv. Mater.*, 2023, **35**(39), 2301929.

20 Y. Xiao, H. Wang, Z. Xie, M. Shen, R. Huang, Y. Miao, G. Liu, T. Yu and W. Huang, NIR TADF emitters and OLEDs: challenges, progress, and perspectives, *Chem. Sci.*, 2022, **13**(31), 8906–8923.

21 Z. Wang, X. Zou, Y. Xie, H. Zhang, L. Hu, C. C. S. Chan, R. Zhang, J. Guo, R. T. K. Kwok, J. W. Y. Lam, I. D. Williams, Z. Zeng, K. S. Wong, C. D. Sherrill, R. Ye and B. Z. Tang, A nonconjugated radical polymer with stable red luminescence in the solid state, *Mater. Horiz.*, 2022, **9**, 2564–2571.

22 L. Peng, J. Lv, S. Xiao, Y. Huo, Y. Liu, D. Ma, S. Ying and S. Yan, High-performance non-doped near ultraviolet OLEDs with the EQE $\sim$ 6% and CIEy $\sim$ 0.03 from high-lying reverse intersystem crossing, *Chem. Eng. J.*, 2022, **450**, 138339.

23 Z. Huang, H. Xie, J. Miao, Y. Wei, Y. Zou, T. Hua, X. Cao and C. Yang, Charge Transfer Excited State Promoted Multiple Resonance Delayed Fluorescence Emitter for High-Performance Narrowband Electroluminescence, *J. Am. Chem. Soc.*, 2023, **145**(23), 12550–12560.

24 B. Lei, Z. Huang, S. Li, J. Liu, Z. Bin and J. You, Medium-Ring Strategy Enables Multiple Resonance Emitters with Twisted Geometry and Fast Spin-Flip to Suppress Efficiency Roll-Off, *Angew. Chem., Int. Ed.*, 2023, **62**(12), 202218405.

25 S. Luo, J. Wang, N. Li, X. F. Song, X. Wan, K. Li and C. Yang, Regulation of Multiple Resonance Delayed Fluorescence *via* Through-Space Charge Transfer Excited State towards High-Efficiency and Stable Narrowband Electroluminescence, *Angew. Chem., Int. Ed.*, 2023, **62**(49), 202310943.

26 Q. Wang, Y. Xu, T. Huang, Y. Qu, J. Xue, B. Liang and Y. Wang, Precise Regulation of Emission Maxima and Construction of Highly Efficient Electroluminescent Materials with High Color Purity, *Angew. Chem., Int. Ed.*, 2023, **62**(19), 202301930.

27 Y. Sano, T. Shintani, M. Hayakawa, S. Oda, M. Kondo, T. Matsushita and T. Hatakeyama, One-Shot Construction of BN-Embedded Heptadecacene Framework Exhibiting Ultra-narrowband Green Thermally Activated Delayed Fluorescence, *J. Am. Chem. Soc.*, 2023, **145**(21), 11504–11511.

28 G. Meng, H. Dai, J. Zhou, T. Huang, X. Zeng, Q. Wang, X. Wang, Y. Zhang, T. Fan, D. Yang, D. Ma, D. Zhang and L. Duan, Wide-range color-tunable polycyclo-heteraborin multi-resonance emitters containing B-N covalent bonds, *Chem. Sci.*, 2023, **14**(4), 979–986.

29 Y. Liu, B. Du, X. Han, X. Wu, H. Tong and L. Wang, Intramolecular-locked triazatruxene-based thermally activated delayed fluorescence emitter for efficient solution-processed deep-blue organic light emitting diodes, *Chem. Eng. J.*, 2022, **446**, 137372.

30 Y. Liu, Y. Xie, Y. Cheng, X. Tian, L. Hua, S. Ying, S. Yan and Z. Ren, High-efficiency emissive dendritic phosphorescent iridium (III) complex with thermally activated delayed fluorescence molecules as functional light-harvesting moieties, *Chem. Eng. J.*, 2023, **455**, 140747.

31 H. Chen, T. Fan, G. Zhao, D. Zhang, G. Li, W. Jiang, L. Duan and Y. Zhang, A Simple Molecular Design Strategy for Pure-Red Multiple Resonance Emitters, *Angew. Chem., Int. Ed.*, 2023, **62**(20), 202300934.

32 D. Chen, F. Tenopala-Carmona, J. A. Knöller, A. Mischok, D. Hall, S. Madayanad Suresh, T. Matulaitis, Y. Olivier, P. Nacke, F. Gießelmann, S. Laschat, M. C. Gather and E. Zysman-Colman, Mesogenic Groups Control the Emitter Orientation in Multi-Resonance TADF Emitter Films, *Angew. Chem., Int. Ed.*, 2023, **62**(16), 202218911.

33 Y. Hu, Z. Wang, X. Jiang, X. Cai, S.-J. Su, F. Huang and Y. Cao, One-step synthesis of cyclic compounds towards easy room-temperature phosphorescence and deep blue thermally activated delayed fluorescence, *Chem. Commun.*, 2018, **54**(56), 7850–7853.

34 S. Izumi, A. Nyga, P. de Silva, N. Tohnai, S. Minakata, P. Data and Y. Takeda, Revealing Topological Influence of Phenylenediamine Unit on Physicochemical Properties of Donor-Acceptor-Donor-Acceptor Thermally Activated Delayed Fluorescent Macrocycles, *Chem.–Asian J.*, 2020, **15**(23), 4098–4103.

35 D. W. Zhang, J. M. Teng, Y. F. Wang, X. N. Han, M. Li and C. F. Chen, D-pi*-A type planar chiral TADF materials for efficient circularly polarized electroluminescence, *Mater. Horiz.*, 2021, **8**(12), 3417–3423.

36 X. Wang, Y. Zhang, H. Dai, G. Li, M. Liu, G. Meng, X. Zeng, T. Huang, L. Wang, Q. Peng, D. Yang, D. Ma, D. Zhang and L. Duan, Mesityl-Functionalized Multi-Resonance Organoboron Delayed Fluorescent Frameworks with Wide-Range Color Tunability for Narrowband OLEDs, *Angew. Chem., Int. Ed.*, 2022, **61**(38), 202206916.

37 J. Liu, Y. Zhu, T. Tsuboi, C. Deng, W. Lou, D. Wang, T. Liu and Q. Zhang, Toward a BT 2020 green emitter through

a combined multiple resonance effect and multi-lock strategy, *Nat. Commun.*, 2022, **13**(1), 4876.

38 Z. Zhao, K. Liu, Y. Liu, Y. Guo and Y. Liu, Intrinsically flexible displays: key materials and devices, *Natl. Sci. Rev.*, 2022, **9**(6), nwac090.

39 K.-G. Lim, T.-H. Han and T.-W. Lee, Engineering electrodes and metal halide perovskite materials for flexible/stretchable perovskite solar cells and light-emitting diodes, *Energy Environ. Sci.*, 2021, **14**(4), 2009–2035.

40 D. Zhang, T. Huang and L. Duan, Emerging aelf-amissive technologies for flexible displays, *Adv. Mater.*, 2020, **32**(15), e1902391.

41 S. Lee, E. H. Kim, S. Yu, H. Kim, C. Park, T. H. Park, H. Han, S. W. Lee, S. Baek, W. Jin, C. M. Koo and C. Park, Alternating-Current MXene Polymer Light-Emitting Diodes, *Adv. Funct. Mater.*, 2020, **30**(32), 2001224.